Inorganic Chemistry Research

Article

Oxidative Addition Reactions of Binuclear Organoplatinum Complexes with Ditopic Ligands

Matthew S. McCready and Richard J. Puddephatt*

Department of Chemistry, University of Western Ontario, London, Canada N6A 5B7

Received: February 2, 2022; Accepted: April 6, 2021

Cite This: *Inorg. Chem. Res.* **2022**, *6*, 58-67. DOI: 10.22036/icr.2022.327842.1125

Abstract: The chemistry of *bis*[dimethylplatinum(II)] complexes of four ditopic ligands based on anthracene [1,8-$C_{14}H_8$(N=CH-2-C_5H_4N)$_2$, **L1**, and 1,8-$C_{14}H_8$(CC-4-C_6H_4-N=CH-2-C_5H_4N)$_2$, **L2**] or 2,7-di-*t*-butyl-9,9-dimethyl-xanthene [4,5-$C_{23}H_{28}O$(N=CH-2-C_5H_4N)$_2$, **L3**, and [4,5-$C_{23}H_{28}O$(C(=O)NH-4-C_6H_4-N=CH-2-C_5H_4N)$_2$, **L4**] backbones. Each complex [($PtMe_2$)$_2$(**L1**)] - [($PtMe_2$)$_2$(**L4**)] reacted with MeI to give the corresponding platinum(IV) complex [($PtIMe_3$)$_2$(**L1**)] - [($PtIMe_3$)$_2$(**L4**)] as a mixture of two isomers which equilibrated slowly at room temperature. The complex [($PtMe_2$)$_2$(**L3**)] also underwent oxidative addition with $PhCH_2Br$, I_2 or $HgBr_2$ to give [($PtBrMe_2CH_2Ph$)$_2$(**L3**)], [(PtI_2Me_2)$_2$(**L3**)] or [($PtBrMe_2$)$_2$(Hg)(**L3**)] respectively, the last containing a Pt-Hg-Pt unit. Finally, the complexes [($PtIMe_3$)$_2$(**L3**)] and [($PtIMe_3$)$_2$(**L4**)] reacted with silver triflate and pyrazine ($C_4H_4N_2$) to give the complexes [($PtMe_3$)$_2$($C_4H_4N_2$)(**L3**)][O_3SCF_3]$_2$ and [($PtMe_3$)$_2$($C_4H_4N_2$)(**L4**)][O_3SCF_3]$_2$, respectively, each of which contains a bridging pyrazine ligand

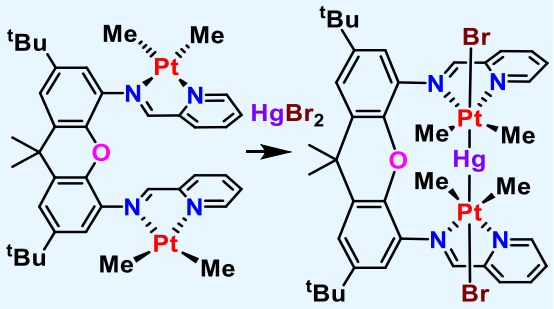

Keywords: Oxidative addition, Platinum, Binuclear

This paper is published in memory of Professor Mehdi Rashidi in appreciation of his great contributions to organoplatinum chemistry.

1. INTRODUCTION

There is continuing interest in the synthesis and properties of binuclear transition metal complexes for potential applications in catalysis, functional molecular materials or pharmaceutical compounds.[1-11] If a ditopic ligand holds two separate transition metal centres in close proximity, one metal centre can significantly affect the reactivity of the other, and the introduction of donor ligands as substituents at the 1,8-positions of anthracene or 4,5-positions of xanthene provides a suitable scaffold to study such effects.[12,13] One complication in anthracene derivatives is that C-H bond activation at C(9) may occur, as illustrated in Scheme 1.[14,15] This problem is avoided in xanthene based ligands, as illustrated in Scheme 2.[16-19] The cyclic ligand in ***A*** (Scheme 2) has the most rigid structure, while the open ligands in ***B***–***D*** are more flexible and can accommodate a wider range of inter-metal distances.[18,19] The conformation of individual bidentate ligands can be mutually *anti* (complex ***C***) or *syn* (complex ***D***) and a bridging ligand can be accommodated (complex ***D***) (Scheme 2).

Oxidative addition is a key reaction in many catalytic cycles and so it has been studied in detail, especially using organoplatinum complexes. [20-22] This article describes studies of oxidative addition to binuclear dimethylplatinum(II) complexes with ditopic ligands similar to those in Scheme 2, especially in a search for bimetallic reactivity. In the context of this special issue for Mehdi Rashidi, we note his expertise in oxidative addition chemistry, including with diplatinum complexes of several types.[20,22-24] On a personal note, we (MR and RJP) enjoyed publishing 38 papers together over the 37 year period from 1976-2013, beginning with his Ph.D. studies in Liverpool, continuing with occasional sabbatical visits to Canada, and interspersed with several long distance collaborations.[25-27]

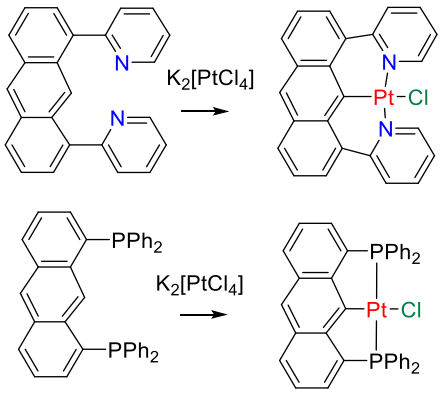

Scheme 1. Some reactions of anthracene based ligands involving activation of the C(9)-H bond.

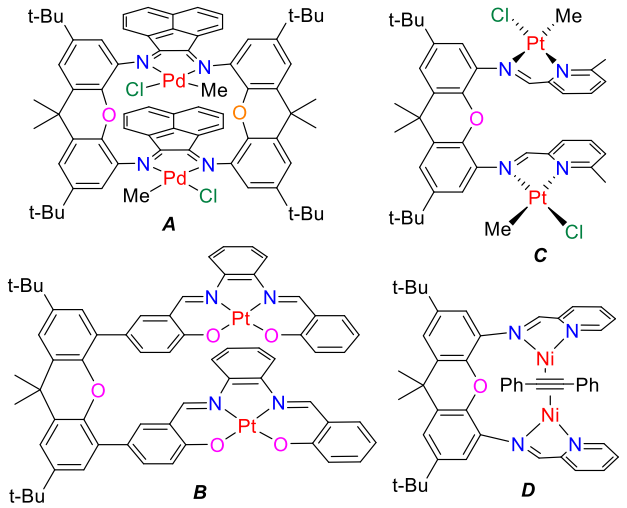

Scheme 2. Some bimetallic complexes based on a xanthene ligand scaffold

2. RESULTS AND DISCUSSION

The ligands **L1**–**L4** used in this work are shown in Scheme 3, of which only **L3** has been reported previously.[18,19] Ligands **L1** and **L3** were prepared simply by condensation of the corresponding diamine derivative of anthracene or xanthene with 2-pyridyl carboxaldehyde, while the final step in the syntheses of **L2** and **L4** are shown in Scheme 4. While the anthracene and xanthene units are rigid, the diimine units can rotate about the aryl-nitrogen bonds and adopt conformations in which the diimine units are mutually *syn* or *anti*. The *anti* conformer is expected to have effective C_2 symmetry while the *syn* conformer is expected to have effective C_s symmetry. Rapid rotation is expected to interconvert the conformers in most cases but, if rotation is slow, the conformation of the ligands **L3** and **L4** could be distinguished by the presence of one or two resonances for the CMe_2 groups for the *anti* or *syn* conformer, respectively, in the ^{1}H NMR spectra. The ligand **L3** gave single sharp resonance in the ^{1}H NMR spectra for the CMe_2 group, but all resonances for **L4** were broad, probably as a result of restricted rotation about the amide units, arising in part from intramolecular hydrogen bonding (Scheme 3). Exchange between possible *syn* and *anti* conformers is expected to be slowed by the hydrogen bonding.

Each of the ligands **L1**–**L4** gave a bis(dimethylplatinum) derivative **1**–**4** on reaction with $[Pt_2Me_4(\mu\text{-}SMe_2)_2]$ with displacement of dimethylsulfide groups (Scheme 5).[28,29] In each case, the ^{1}H NMR spectra contained two methylplatinum resonances with coupling constants ^2J(PtH) *ca.* 85 Hz, in the range expected for platinum(II) complexes,[27-30] as well as the expected ligand resonances (Figure 1). Coupling of ^{195}Pt to both the imine and *ortho* pyridyl protons confirms the site of ligand coordination. The observation of a single resonance for the CMe_2 protons of the xanthene derivatives **3** and **4** is consistent

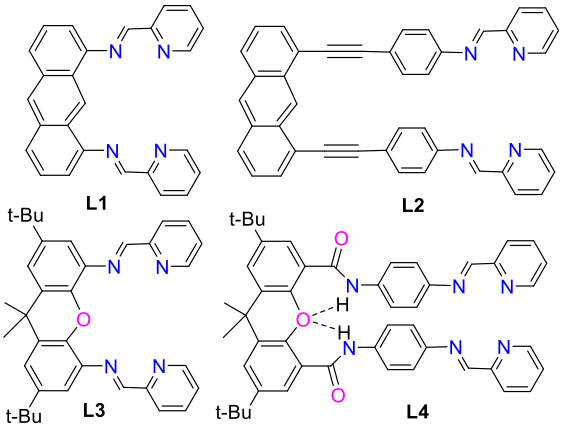

Scheme 3. The four ditopic ligands **L1**–**L4**.

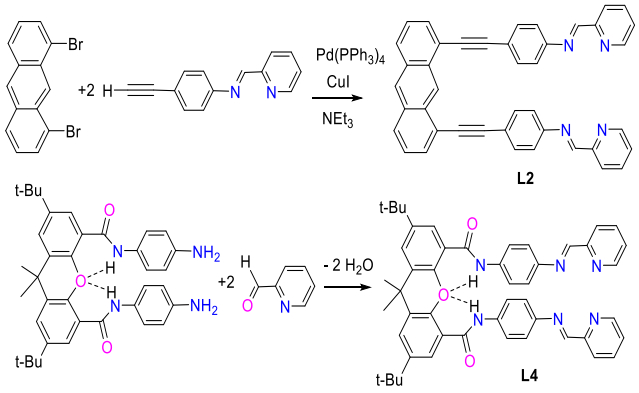

Scheme 4. Synthesis of **L2** and **L4**.

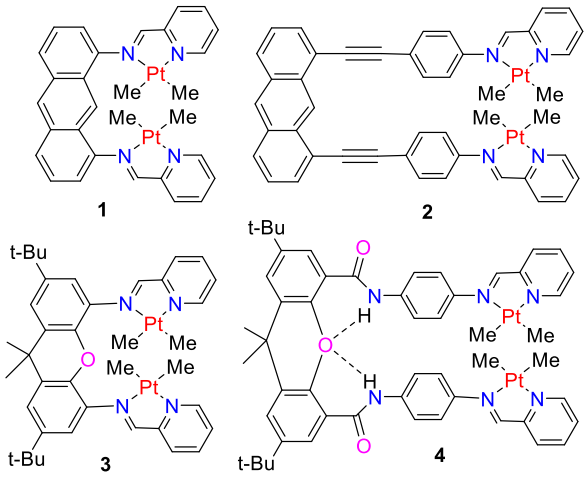

Scheme 5. The bis(dimethylplatinum) complexes **1**–**4**.

with the *anti* conformation of the two diamine groups in each case (Figure 1). Complexes **2**–**4** were stable in solution, but complex **1** decomposed over a period of about one day, with precipitation of a black solid which was insoluble in all common organic solvents. When this reaction was monitored by ^{1}H NMR spectroscopy, the resonances for **1** slowly decayed but no new resonances

appeared. The nature of the reaction giving the black solid is therefore not known, though we note the complications observed with other anthracene based ligands (Scheme 1) and the higher stability of complex **2**, in which the platinum units are further removed from the anthracene backbone.

Each of the complexes **1**– **4** reacted rapidly with methyl iodide to give the corresponding platinum(IV) complexes $[(PtIMe_3)_2(\mathbf{L1})]$-$[(PtIMe_3)_2(\mathbf{L4})]$, **5**–**8**, respectively (Scheme 6). The syntheses were straightforward except in the case of complex **5**, when a black solid was also formed, probably the same insoluble solid as was observed in the synthesis of complex **1**. Complex **5** was formed in higher yield by oxidative addition of methyl iodide to $[Pt_2Me_4(\mu\text{-}SMe_2)_2]$ followed by reaction of the platinum(IV) complex formed with ligand **L1**. Both of the xanthene-based complexes **7** and **8** were characterized crystallographically and the structures are shown in Figures 2 and 3.

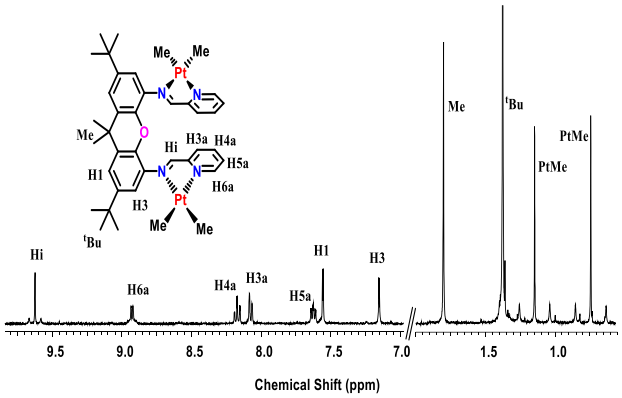

Figure 1. ^{1}H NMR spectrum of $[(PtMe_2)_2(\mathbf{L3})]$, **3**.

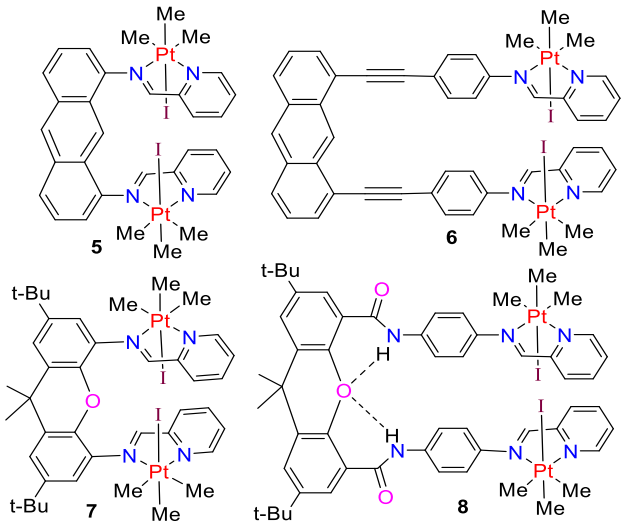

Scheme 6. The complexes $[(PtIMe_3)_2(\mathbf{L1})]$-$[(PtIMe_3)_2(\mathbf{L4})]$, **5**–**8**

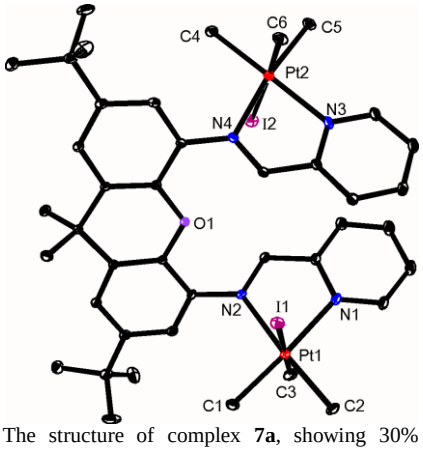

Figure 2. The structure of complex **7a**, showing 30% probability ellipsoids.

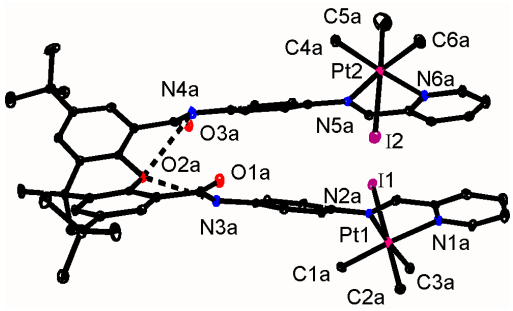

Figure 3. The structure of one of the two independent molecules of complex **8a**, showing 30% probability ellipsoids.

The structure of complex **7** is shown in Figure 2. The lattice also contained disordered molecules of solvent CH_2Cl_2 and benzene, and there was rotational disorder of a *t*-butyl group. In the structure of **8**, there were two independent molecules and an acetone solvate molecule. There are two notable features of the structures. The first is that Me-I disorder was observed in both structures, with the major isomer shown in Figures 2 and 3. For complex **7**, the major isomer was refined to have 95% abundance and can be described as the isomer with effective C_2 symmetry, **7a**. The minor isomer, having only 5% abundance, is formed by exchange of the atoms C(6) and I(2) at the Pt(2) center and is the isomer with effective C_s symmetry **7b**. For complex **8**, the independent molecule containing Pt(3)/Pt(4) does not display Me/I disorder but the molecule containing Pt(1)/Pt(2), shown in Figure 3, displays C(5a)/I(2) disorder with the major isomer having 97% abundance. The Pt(3)/Pt(4) molecule and the major Pt(1)/Pt(2) molecule both have effective C_2 symmetry, **8a**, while the minor isomer has effective C_s symmetry **8b**. The second notable feature in the structures concerns folding of the xanthene backbone, measured by the angle between the planes of the two benzene rings. For complex **7**, this angle is 6°, while for **8** the two independent molecules have very different fold angles, being 3° in the Pt(3)/Pt(4) molecule but 34° in the Pt(1)/Pt(2) molecule shown in Figure 3. It

could be argued that differences in NH··O hydrogen bonding involving the xanthene oxygen atom might affect the degree of folding, but the corresponding distances (N··O 2.86 and 2.92 Å in the Pt(1)/Pt(2) molecule and 2.76 and 2.93 Å in the Pt(3)/Pt(4) molecule) are similar and so do not provide an explanation. It is likely that the flat and folded xanthene structures are similar in energy and would undergo fast flexing in solution. Easy access to the flat xanthene structure is needed for effective C_2 symmetry of **7a** and **8a**.

The ^{1}H NMR spectra of the complexes **6**–**8** were consistent with the presence of two isomers in each case, but the resonances of individual isomers were often overlapped, thus making full assignments challenging. The spectra of xanthene derivatives **7** and **8** were instructive. For these complexes, the initial reaction with methyl iodide gave roughly equal amounts of isomers **7a** and **7b** or **8a** and **8b**, but then slow isomerization of **7b** to **7a** or **8b** to **8a** occurred over several days in solution. Figure 4 shows spectra of complex **7**, as a freshly prepared sample and after several days in solution. Little could be learned from the methylplatinum or *t*-butyl resonances which had very similar chemical shifts for both isomers, but the resonances of the Me_2C unit of the xanthene unit were very informative. Complex **7a** has effective C_2 symmetry and so the two methyl groups are symmetry equivalent and give a single resonance, whereas **7b** has C_s symmetry and the two methyl groups are not equivalent and give two equal intensity singlet resonances. Thus, as **7b** decays and **7a** grows, the singlet Me_2C resonance increases in intensity and the two singlets on either side decay. In the final equilibrium mixture the ratio of **7a**:**7b** is about 10:1, consistent with the approximate ratio present in the disordered crystal.

The chemistry for complex **7** is summarized in Scheme 7. The oxidative addition of methyl iodide to complex **3** is not selective and gives a roughly equal mixture of isomers **7a** and **7b**. The complexes with the *anti* conformation of the bidentate ligands is expected to be most stable, as found in the structure determination (Figure 2), because it has less steric repulsion between the axial substituents of the platinum(IV) centers. Complex **7a** has effective C_2 symmetry and will give a singlet resonance in the ^{1}H NMR spectrum for the Me_2C protons. Complex **7b**, as the *anti* conformer has no symmetry but rotation about the aryl-N bonds is expected to lead to rapid exchange with the less stable *syn* conformer **7b'**, which has effective C_s symmetry, and so will give two singlet resonances in the ^{1}H NMR spectrum for the Me_2C protons. Exchange between **7a** and **7b** is expected to occur by dissociation of an iodide ligand to give a 5-coordinate platinum(IV) center, followed by methyl migration and recoordination of iodide on the opposite face, and this is typically slow in related complexes.[20,31-33]

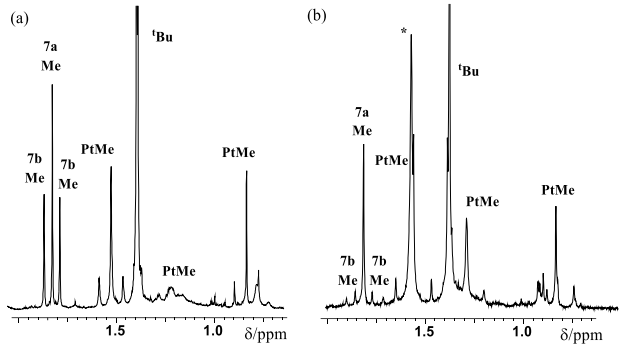

Figure 4. ^{1}H NMR spectra of complex **7** in the aliphatic region. (a) freshly prepared sample, containing about equal amounts of isomers **7a** and **7b**; (b) equilibrium mixture of isomers, mostly **7a**.

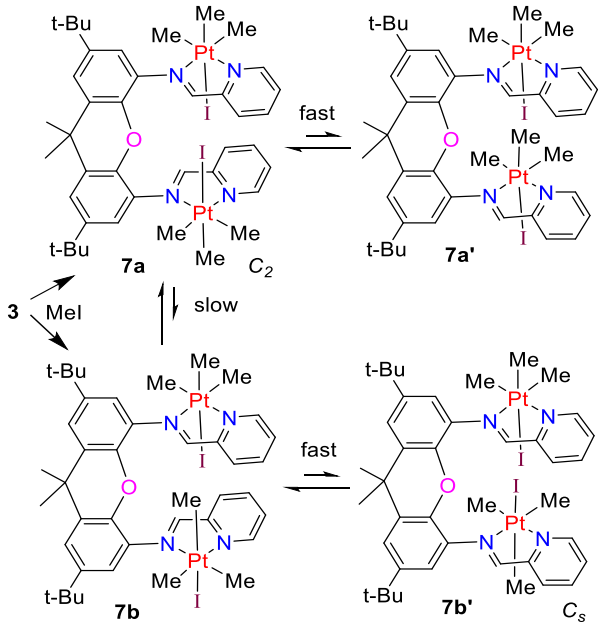

Scheme 7. Isomers and conformers of complex **7** and their interconversion

The oxidative addition of benzyl bromide to complex **3** occurred more selectively to give a single isomer [$Pt_2Br_2Me_4(CH_2Ph)_2$(**L3**)], **9**, whose ^{1}H NMR spectrum contained a single resonance for the CMe_2 protons, indicative of the C_2 isomer formed by *trans* oxidative addition at both platinum centers (Scheme 8).[27] A single "AB" quartet was observed for the $PtCH^AH^BPh$ protons [δ 2.77, ^2J(HH) = 9 Hz, ^2J(PtH) = 102 Hz, CH^A; δ 3.34, ^2J(HH) = 9 Hz, ^2J(PtH) = 96 Hz, CH^B]. Similarly, iodine reacted with complex **3** very largely by *trans* oxidative addition to give complex **10**,[34] and the ^{1}H NMR spectrum indicated the C_2 isomer with *anti* conformation of the bidentate ligands (Scheme 8, Figure 5). In this case the structure was confirmed by X-ray structure determination (Figure 6).

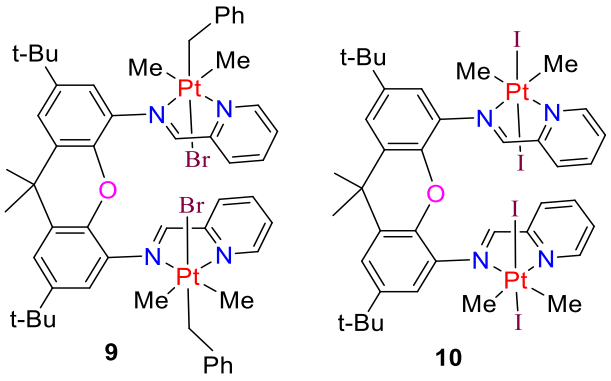

Scheme 8. The structures of complexes **9** and **10**

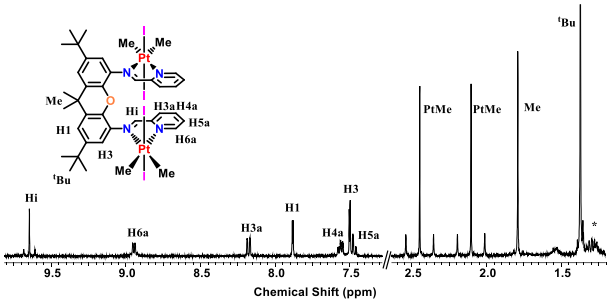

Figure 5. ^{1}H NMR spectrum of [$Pt_2I_4Me_4$(**L3**)], **10**, in CD_2Cl_2; * indicates pentane impurity.

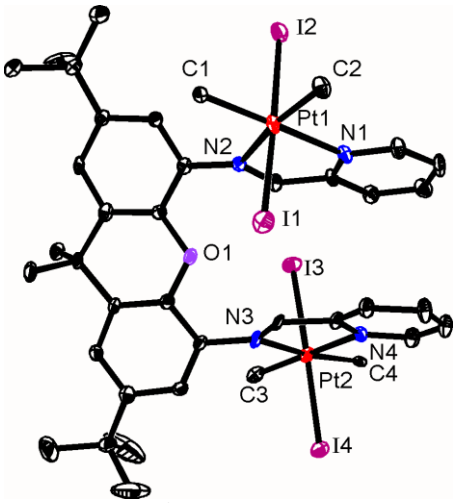

Figure 6. The structure of complex **10**, showing 30% probability ellipsoids.

Several attempts were made to prepare complexes with ligands bridging between the two platinum centers, but these proved challenging. For example, attempts to abstract one halide ion from complexes **5**–**9** to form a cation complex, with the remaining halide acting as a bridging ligand, failed to yield pure compounds. However, two systems were successful and are described below. Mercury(II) bromide reacted cleanly with complex **3** to give [($PtBrMe_2$)$_2$(μ-Hg)(**L3**)], **11**, presumably in a two step oxidative addition, though the intermediate could not be detected (Scheme 9).[35-38] Single crystals of **11** were not obtained but it is convincingly characterized by its ^{1}H NMR spectrum (Figure 7). Two methylplatinum resonances were observed at δ = 1.01 and 1.51, each with ^2J(PtH) = 62 Hz and ^3J(HgH) = 12 Hz. The structure is defined as having C_s symmetry, with *syn* orientation of the two pyridyl-imine ligands, by the observation of two well separated singlet resonances for the Me_2C group (Figure 7).

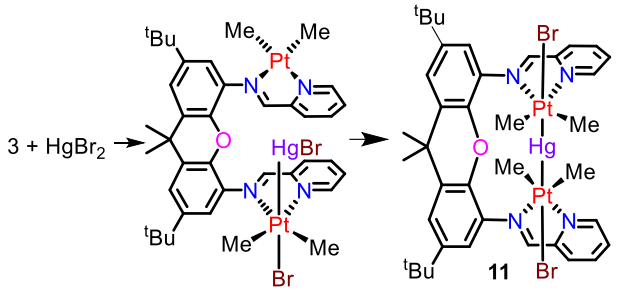

Scheme 9. The oxidative addition of mercuric bromide to give complex **11**.

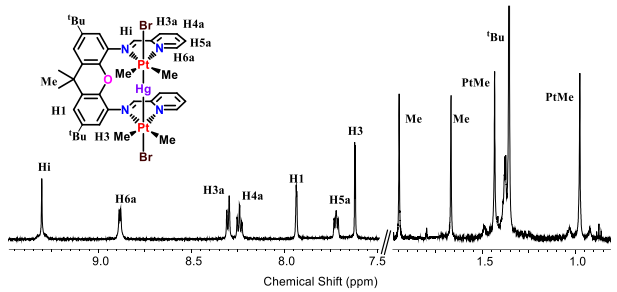

Figure 7. ^{1}H NMR spectrum of complex **11** in acetone-d_6.

Two complexes with bridging pyrazine ligands [($PtMe_3$)$_2$(μ-$C_4H_4N_2$)(**L3**)], **12**, and [($PtMe_3$)$_2$(μ-$C_4H_4N_2$)(**L4**)], **13**, were prepared by reaction of the corresponding complex **7** or **8** with silver triflate and pyrazine, according to Scheme 10. In the ^{1}H NMR spectra, both **12** and **13** gave three methylplatinum resonances and two singlet resonances for the Me_2C protons, as expected for the isomer with C_s symmetry having the *syn* orientation of the pyridyl-imine ligands. Complex **13** gave a single resonance for the four protons of the bridging pyrazine ligand (δ = 8.54, 4H), while complex **12** gave two equal intensity singlet resonances (Figure 8, δ = 8.20 and 8.75, each 2H). This indicates that there is restricted rotation about the PtNNPt axis in complex **12**, in which the pyrazine is much closer to the backbone xanthene group than in **13**, and the two pyrazine resonances for **12** are attributed to the protons directed towards or away from the xanthene unit. The crystal structure of complex **12** confirms the structure proposed from the NMR data and shows considerable bowing of the Pt_2(μ-pyrazine) unit (Figure 9).

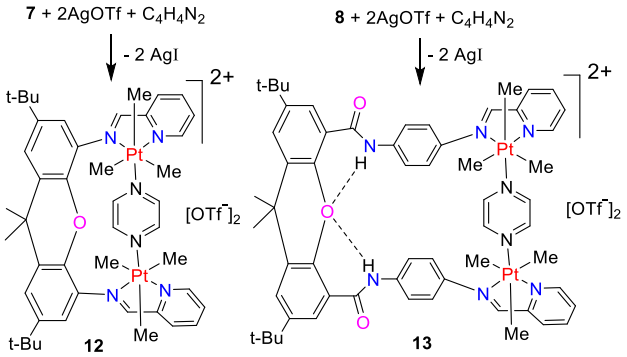

Scheme 10. The synthesis of complexes **12** and **13**.

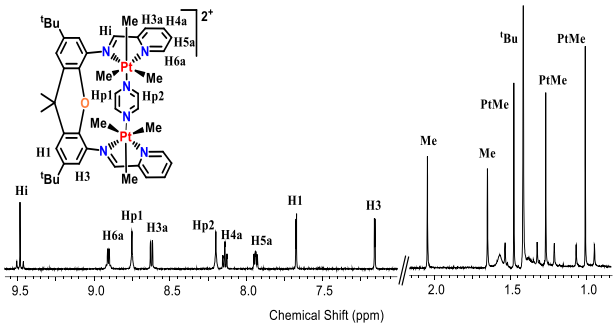

Figure 8. ^{1}H NMR spectrum of the pyrazine bridged diplatinum(IV) complex **12** in CD_2Cl_2.

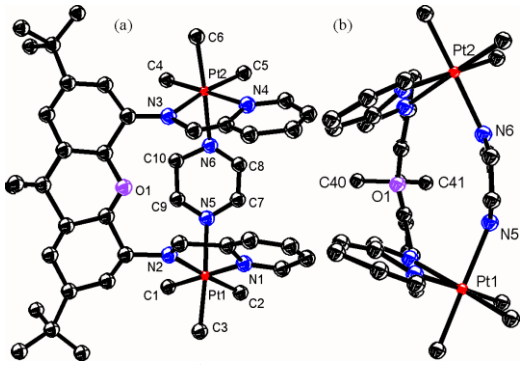

Figure 9. The structure of the dicationic complex **12**; (a) a view orthogonal to the pyrazine ligand, showing non-equivalence of atoms C(7),C(8) versus C(9),C(10); (b) a view showing the bowing of the Pt_2(μ-pyrazine) unit and the non-equivalence of methyl groups at C(40) and C(41) (*t*-Bu groups omitted for clarity).

DFT calculations (see experimental for details) were carried out on selected complexes to gain further insight into some of the above chemistry. In particular, it is noteworthy that the structurally characterized complexes without bridging groups (Figures 2,3,6) adopt the *anti* conformation of the pyridyl-imine ligands while those with bridging ligands adopt the *syn* conformation (Scheme 9, Figure 9). For the dimethylplatinum(II) complexes **1** and **3**, there appear to be no great steric effects and the two arms of the ditopic ligands align roughly parallel to one another. The calculation predicts that the *anti* rotamer is favored by 20 and 33 kJ mol^{-1} for **1** and **3** respectively (Figure 10).

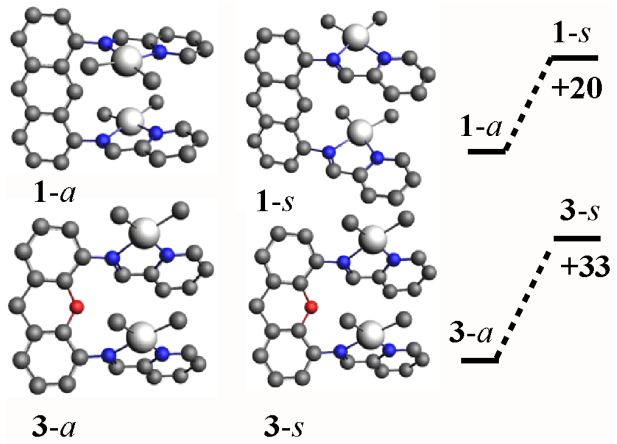

Figure 10. Calculated structures and relative energies (kJ mol^{-1}) of the *anti* and *syn* conformers for complexes **1** and **3**. The alkyl substituents of the xanthene ligand in **3** are omitted in the calculations.

For the octahedral platinum(IV) complexes **7**, there is clearly greater steric hindrance for the *syn* rotamers (**7a'**, **7b'**), in which the platinum centers lie on the same side of the xanthene, than for the *anti* rotamers (**7a**, **7b**), in which they lie on opposite sides (Figure 11). The energy difference between rotamers is calculated as 67 and 34 kJ mol^{-1} for isomers **7a** and **7b** respectively, while the C_2 isomer **7a** is calculated to be more stable than the C_s isomer **7b** by 16 kJ mol^{-1}. These values are consistent with the observed data (Scheme 7, Figure 4).

The calculated structures and relative energies of the possible isomers of the bridged complex **11** and **12** are shown in Figure 12. For these complexes, the *syn* C_s symmetric isomers are found experimentally and the theory successfully predicts the observed structures, with **11** and **12** more stable by 44 and 49 kJ mol^{-1} than the alternative C_2 symmetric isomers **11**-*anti* and **12**-*anti*, respectively.

In summary, the ligands **L1**–**L4** are all capable of supporting diplatinum complexes and significant new chemistry has been discovered from their study. The anthracene-based ligands **L1** and **L2** give sparingly soluble complexes, which limits their usefulness, and the platinum complexes of ligand **L1** have low thermal stability. The xanthene-based ligands **L3** and **L4** have greater potential, since the facile introduction of alkyl substituents leads to higher solubility of the platinum complexes. In addition, the Me_2C group gives a valuable method of distinguishing between *syn* and *anti* conformers of the ditopic ligands by NMR spectroscopy, provided that rotation is not too rapid. In general, the unbridged complexes are shown to be more stable in the *anti* conformation, while the bridged complexes prefer the *syn* conformation of the ditopic ligands. The ligands are flexible and either conformation can accommodate a range of Pt··Pt distances. In complexes

of the ligand **L3**, the Pt··Pt distances from structure determinations are 7.75
and 7.78 Å in complexes **7a** and **10**, with *anti* conformation, and 6.73 Å in complex **12**, with *syn* conformation. From DFT calculations, the Pt··Pt distance is predicted to be 5.24 Å in the dimethylplatinum(II) complex **3** and 5.27 Å in the mercury-bridged complex **11**, which have *anti* and *syn* conformations of the ditopic ligand respectively. Complexes of the type described above comprise a significant addition to the diplatinum complexes described earlier[20,22,39,40] and similar compounds should be excellent candidates for bimetallic catalysis.

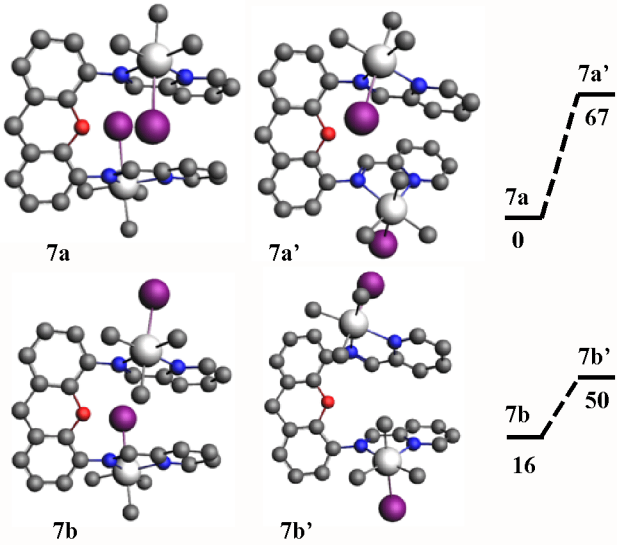

Figure 11. Calculated structures and relative energies (kJ mol^{-1} with respect to most stable form **7a**) of isomers and conformers of complex **7**.

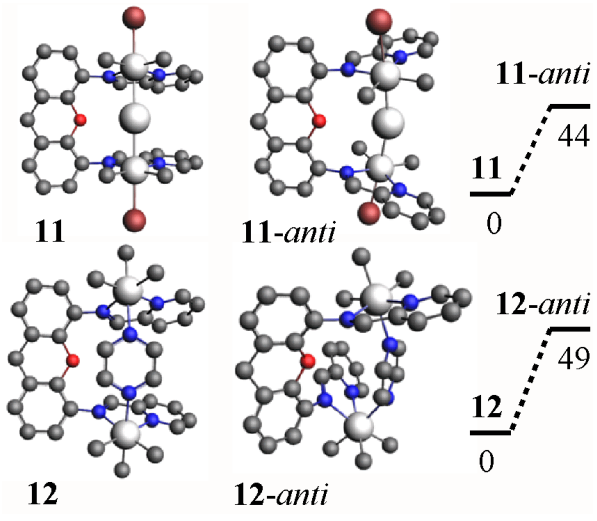

Figure 12. Calculated structures of the C_s and C_2 isomers of complexes **11** and **12**, and relative energies (kJ mol^{-1} with respect to the more stable *syn* C_s isomer).

3. EXPERIMENTAL

The complex $[Pt_2Me_4(\mu\text{-}SMe_2)_2]$ was prepared according to the literature method.[28] NMR spectra were recorded at ambient temperature, unless otherwise noted, by using Varian Mercury 400 or Varian Inova 400 or 600 spectrometers. ^{1}H chemical shifts are reported relative to TMS (^{1}H). Complete assignment of each compound was aided by ^{1}H-^{1}H NOESY, ^{1}H-^{13}C{^{1}H}-HSQC and ^{1}H-^{1}H gCOSY experiments. Mass spectrometric analysis was carried out using an electrospray PE-Sciex Mass Spectrometer (ESI-MS) coupled with a TOF detector. X-ray data were collected at 150K with ω and φ scans on a Bruker Smart Apex II diffractometer using graphite-monochromated Mo-Kα radiation (λ = 0.71073 Å). A suitable crystal was coated in Paratone oil and mounted on a glass fiber loop. Unit cell parameters were calculated and refined from the full data set. Cell refinement and data reduction were performed using the Bruker software.[41,42] All structures were solved by direct methods and refined by full-matrix least-squares techniques.[43,44] The hydrogen atoms were placed in calculated positions and refined using the riding model. Details of individual structures are given in the cif files (CCDC 2145542-2145544). The DFT calculations were carried out using the BLYP functional, with double-zeta basis set and first-order scalar relativistic corrections, as implemented in ADF-2020.[45-47] Details of the calculated ground state structures are given in the Supporting Information.

N^1,N^8-bis(pyridin-2-ylmethylene)anthracene-1,8-diamine, L1. To a solution of 1,8-diaminoanthracene (0.50 g, 2.39 mmol) in toluene (10 mL) was added 2-pyridinecarboxaldehyde, (0.455 mL, 4.78 mmol). The mixture was heated under reflux using a Dean-Stark apparatus for 12 h., the solvent was removed under vacuum, and the product was recrystallized from acetone/pentane. Yield 72%. NMR in $CDCl_3$: δ(^{1}H) 7.16 (d, ^3J(HH) = 7 Hz, 2H, H4), 7.45 (dd, ^3J(HH) = 5 Hz, 7 Hz, 2H, H5a), 7.52 (t, ^3J(HH) = 8 Hz, 2H, H3), 7.81 (t, ^3J(HH) = 7 Hz, 2H, H4a), 7.97 (d, ^3J(HH) = 8 Hz, 2H, H2), 8.48 (d, ^3J(HH) = 7 Hz, 2H, H3a), 8.48 (s, 1H, H10), 8.76 (d, ^3J(HH) = 5 Hz, 2H, H6a), 8.79 (s, 2H, Hi), 9.44 (s, 1H, H9). EI-MS: $[C_{26}H_{18}N_4]^+$ Calc. m/z = 386; Found m/z = 386. Anal. Calc. for $C_{26}H_{18}N_4$•0.5CH_2Cl_2(%): C, 74.46; H, 4.48; N: 12.94%. Found: C, 74.21; H, 4.46; N, 13.06%.

4,4'-(Anthracene-1,8-diylbis(ethyne-2,1-diyl))-bis(*N*-(pyridin-2-ylmethylene)aniline), L2. A mixture of 1,8-dibromoanthracene (0.250 g, 0.745 mmol), 4-ethynyl-*N*-(pyridine-2-ylmethylene)aniline (0.328 g, 1.59 mmol), $[Pd(PPh_3)_4]$ (91 mg) and CuI (15 mg) in dry Et_3N (20 mL) was heated under reflux for 24h. in an atmosphere of dry N_2. The solvent was removed under vacuum and the resultant brown solid was extracted with dichloromethane and purified by chromatography using a silica gel column and ethyl acetate/hexanes as eluent to yield the product as a yellow solid in 68% yield. NMR in $CDCl_3$: δ(^{1}H) 7.17 (d, ^3J(HH) = 7 Hz, 4H, H2b), 7.31 (dd, ^3J(HH) = 7 Hz, 5 Hz, 2H, H5a), 7.52 (t, ^3J(HH) = 7 Hz, 2H, H3), 7.66 (d, ^3J(HH) = 7 Hz, 4H, H3b), 7.67 (t, ^3J(HH) = 7 Hz, 2H, H4a), 7.84 (d, ^3J(HH) = 7 Hz, 2H, H3a), 8.06 (d, ^3J(HH) = 7 Hz, 2H, H4), 8.10 (d, ^3J(HH) = 7 Hz, 2H, H2), 8.51 (s, 1H, H10), 8.58 (s, 2H, Hi), 8.61 (d, ^3J(HH) = 5 Hz, 2H, H6a), 9.67 (s, 1H, H9). ESI-MS: Calc. for $[C_{42}H_{26}N_4]^+$: m/z = 586.22; determined m/z = 586.22.

2,7-Di-*tert*-butyl-9,9-dimethyl-*N*^{4},*N*^{5}-bis(4-(pyridin-2-ylmethyleneamino)phenyl)-xanthene-4,5-dicarboxamide, L4. A solution of *N*^{4},*N*^{5}-bis(4-aminophenyl)-2,7-di-*tert*-butyl-9,9-dimethyl-xanthene-4,5-dicarboxamide (0.280 g, 0.476 mmol), 2-

pyridinecarboxaldehyde (0.100 mL, 1.044 mmol) and $MeCO_2H$ (0.1 mL) in toluene (15 mL) was heated under reflux using a Dean-Stark apparatus for 8 h. The solvent was removed *in vacuo*, and the resultant solid product was washed with pentane and ether and dried under vacuum. Yield 88%. NMR in $CDCl_3$**:** $\delta(^1H)$ 1.37 (s, 18H, ^{t}Bu), 1.72 (s, 6H, Me), 7.13 (d, ^3J(HH) = 7 Hz, 4H, H3b), 7.29 (dd, ^3J(HH) = 7 Hz, ^3J(HH) = 5 Hz, 2H, H5a), 7.55 (d, ^3J(HH) = 7 Hz, 4H, H2b), 7.61 (s, 2H, H1), 7.67 (t, ^3J(HH) = 7 Hz, 2H, H4a), 7.85 (s, 2H, H3), 8.09 (d, ^3J(HH) = 7 Hz, 2H, H3a), 8.56 (s, 2H, Hi), 8.59 (d, ^3J(HH) = 5 Hz, 2H, H6a), 8.79 (s, 2H, NH). EI-MS: Calc. for $[C_{49}H_{48}N_6O_3]^+$ m/z = 768; determined m/z = 768.

$[Pt_2Me_4(L1)]$, 1. To a stirred solution of $[Pt_2Me_4(\mu\text{-}SMe_2)_2]$ (0.100 g, 0.174 mmol) in toluene (2 mL) was added ligand **L1** (0.067g, 0.174mmol). After 3 h., the solvent was evaporated under vacuum and the purple product was recrystallized from acetone/pentane. Yield: 81%. NMR in acetone-d_6: $\delta(^1H)$ 0.36 (s, ^2J(PtH) = 88 Hz, 6H, PtMe), 0.95 (s, ^2J(PtH) = 86 Hz, 6H, PtMe), 7.30 (d, ^3J(HH) = 7 Hz, 2H, H2), 7.64 (dd, ^3J(HH) = 7 Hz, 9 Hz, 2H, H3), 7.85 (dd, ^3J(HH) = 6 Hz, 8 Hz, 2H, H5a), 8.09 (d, ^3J(HH) = 9 Hz, 2H, H4), 8.15 (d, ^3J(HH) = 8 Hz, 2H, H3a), 8.39 (t, ^3J(HH) = 7 Hz, 2H, H4a), 8.68 (s, 1H, H10), 9.05 (d, ^3J(HH) = 5 Hz, ^3J(PtH) = 25 Hz, 2H, H6a), 9.43 (s, 1H, H9), 9.76 (s, ^3J(PtH) = 33Hz, 2H, Hi). ESI-MS: Calc. for $[C_{30}H_{30}N_4Pt_2Na]^+$ m/z = 859.17; determined m/z = 859.16.

$[Pt_2Me_4(L2)]$, 2. This was prepared similarly but using ligand **L2**, and isolated as a red solid. Yield: 88%. NMR in $CDCl_3$: $\delta(^1H)$ 1.08 (s, ^2J(PtH) = 84 Hz, 6H, PtMe), 1.19 (s, ^2J(PtH) = 86 Hz, 6H, PtMe), 7.25 (d, ^3J(HH) = 8 Hz, 4H, H3b), 7.47 (dd, ^3J(HH) = 7 Hz, 5 Hz, 2H, H5a), 7.52 (t, ^3J(HH) = 7 Hz, 2H, H4a), 7.25 (d, ^3J(HH) = 8 Hz, 4H, H2b), 7.84 (d, ^3J(HH) = 7 Hz, 2H, H3a), 7.92 (d, ^3J(HH) = 8 Hz, 2H, H4), 8.08 (d, ^3J(HH) = 8 Hz, 2H, H2), 8.10 (t, ^3J(HH) = 8 Hz, 2H, H3), 8.52 (s, 1H, H10), 8.85 (d, ^3J(HH) = 5 Hz, ^3J(PtH) = 10 Hz, 2H, H6a), 9.29 (s, ^3J(PtH) = 28 Hz, 2H, Hi), 9.61 (s, 1H, H9). ESI-MS: Calc. for $[C_{46}H_{38}N_4Pt_2Na]^+$ m/z = 1059.23; determined m/z = 1059.22.

$[Pt_2Me_4(L3)]$, 3. This was prepared similarly but using ligand **L3**, and isolated as a purple solid. Yield: 92%. NMR in acetone-d_6: $\delta(^1H)$ 0.74 (s, ^2J(PtH) = 88 Hz, 6H, PtMe); 1.15 (s, ^2J(PtH) = 87 Hz, 6H, PtMe); 1.38 (s, 18H, ^{t}Bu); 1.80 (s, 6H, Me); 7.16 (d, ^4J(HH) = 2 Hz, 2H, H3); 7.56 (d, ^4J(HH) = 2Hz, 2H, H1); 7.62 (dd, ^3J(HH) = 5 Hz, 7 Hz, 2H, H5a); 8.08 (d, ^3J(HH) = 8 Hz, 2H, H3a); 8.17 (dd, ^3J(HH) = 8 Hz, ^3J(HH) = 7 Hz, 2H, H4a); 8.93 (d, ^3J(HH) = 5 Hz, ^3J(PtH) = 23 Hz, 2H, H6a); 9.62 (s, ^3J(PtH) = 34 Hz, 2H, Hi). ESI-MS: Calc. for $[C_{39}H_{50}N_4OPt_2Na]^+$ m/z = 1003.32; determined m/z = 1003.32.

$[Pt_2Me_4(L4)]$, 4. This was prepared similarly but using ligand **L4**, and isolated as a red solid. Yield: 85%. NMR in acetone-d_6: $\delta(^1H)$ 0.95 (s, ^2J(PtH) = 84 Hz, 6H, PtMe), 1.14 (s, ^2J(PtH) = 87 Hz, 6H, PtMe), 1.40 (s, 18H, ^{t}Bu), 1.78 (s, 6H, Me), 7.22 (d, ^3J(HH) = 9 Hz, 4H, H2b), 7.70 (dd, ^3J(HH) = 8 Hz, 5 Hz, 2H, H5a), 7.72 (d, ^3J(HH) = 9 Hz, 4H, H3b), 7.83 (s, 2H, H3), 7.87 (s, 2H, H1), 8.21 (t, ^3J(HH) = 8 Hz, 2H, H4a), 8.22 (d, ^3J(HH) = 8 Hz, 2H, H3a), 9.03 (d, ^3J(HH) = 5 Hz, ^3J(PtH) = 25 Hz, 2H, H6a), 9.58 (s, ^3J(PtH) = 30 Hz, 2H, Hi), 9.92 (s, 2H, NH). ESI-MS: Calc. for $[C_{53}H_{60}N_6O_3Pt_2Na]^+$ m/z = 1241.39; determined m/z = 1241.39.

$[Pt_2I_2Me_6(L1)]$, 5. To a stirred solution of $[Pt_2Me_4(\mu\text{-}SMe_2)_2]$ (0.010 g, 0.0174 mmol) in acetone (5 mL) was added MeI (0.5 mL). After 2 h., the solvent and excess MeI were evaporated under vacuum, the resultant oil was washed with diethyl ether, then dissolved in dry toluene (5 mL). A solution of **L1** (0.0034g, 0.0087mmol) in toluene (2 mL) was added and the mixture was stirred for 1 h. The mixture was filtered to remove some black precipitate, then the solvent was evaporated to give the product as a yellow solid. Yield: 78%. NMR in dmso-d_6: $\delta(^1H)$ 0.44 (s, ^2J(PtH) = 72 Hz, 6H, PtMe), 0.83 (s, ^2J(PtH) = 71 Hz, 6H, PtMe), 1.36 (s, ^2J(PtH) = 71Hz, 6H, PtMe), 6.51 (s, 1H, H9), 7.75 (dd, ^3J(HH) = 7 Hz, 5 Hz, 2H, H5a), 7.87 (d, ^3J(HH) = 8 Hz, 2H, H2), 8.05 (d, ^3J(HH) = 7 Hz, 2H, H3a), 8.25 (t, ^3J(HH) = 8 Hz, 2H, H3), 8.31 (t, ^3J(HH) = 7 Hz, 2H, H4a), 8.58 (d, ^3J(HH) = 8 Hz, 2H, H4), 8.88 (d, ^3J(HH) = 5 Hz, ^3J(PtH) = 19 Hz, 2H, H6a), 8.97 (s, 1H, H10), 9.57 (s, ^3J(PtH) = 30Hz, 2H, Hi). ESI-MS: Calc. for $[C_{32}H_{36}IN_4Pt_2]^+$ m/z = 993.13; determined m/z = 993.13.

$[Pt_2I_2Me_6(L2)]$, 6. To a stirred solution of complex **2** (0.010 g, 0.00965 mmol) in acetone (5 mL) was added MeI (1.5 µL, 0.0195 mmol). After 3 h., the solvent volume was reduced in *vacuo* and pentane was added to precipitate the product as a yellow solid, which was washed with cold pentane and dried under vacuum. Yield: 85%. NMR in $CDCl_3$: $\delta(^1H)$ 1.08 (s, ^2J(PtH) = 84Hz, 6H, PtMe), 1.19 (s, ^2J(PtH) = 86 Hz, 6H, PtMe), 7.25 (d, ^3J(HH) = 8 Hz, 4H, H2b), 7.47 (dd, ^3J(HH) = 7 Hz, 5 Hz, 2H, H5a), 7.52 (t, ^3J(HH) = 7 Hz, 2H, H4a), 7.25 (d, ^3J(HH) = 8 Hz, 4H, H3b), 7.84 (d, ^3J(HH) = 7 Hz, 2H, H3a), 7.92 (d, ^3J(HH) = 8 Hz, 2H, H4), 8.08 (d, ^3J(HH) = 8 Hz, 2H, H2), 8.10 (t, ^3J(HH) = 8 Hz, 2H, H3), 8.52 (s, 1H, H10), 8.85 (d, ^3J(HH) = 5 Hz, ^3J(PtH) = 20Hz, 2H, H6a), 9.29 (s, ^3J(PtH) = 28 Hz, 2H, Hi), 9.61 (s, 1H, H9). ESI-MS: Calc. for $[C_{48}H_{44}N_4Pt_2I_2Na]^+$ m/z = 1343.08; determined m/z = 1343.08.

$[Pt_2I_2Me_6(L3)]$, 7. This was prepared similarly but using complex **3**. Yield: 89%. NMR at 233 K in CD_2Cl_2: $\delta(^1H)$ 0.77 (s, ^2J(PtH) = 72 Hz, 6H, PtMe), 1.21 (br s, ^2J(PtH) = 70 Hz, 6H, PtMe), 1.30 (s, 18H, ^{t}Bu), 1.47 (s, ^2J(PtH) = 71 Hz, 6H, PtMe), 1.74 (s, 6H, Me), 6.94 (d, ^4J(HH) = 2 Hz, 2H, H3), 7.42 (d, ^4J(HH) = 2Hz, 2H, H1), 7.44 (dd, ^3J(HH) = 5 Hz, 7 Hz, 2H, H5a), 7.49 (dd, ^3J(HH) = 8 Hz, ^3J(HH) = 7 Hz, 2H, H4a), 8.44 (d, ^3J(HH) = 8 Hz, 2H, H3a), 8.87 (d, ^3J(HH) = 5 Hz, ^3J(PtH) = 16 Hz, 2H, H6a), 9.92 (s, ^3J(PtH) = 27 Hz, 2H, Hi). ESI-MS: Calc. for $[C_{41}H_{56}IN_4OPt_2]^+$ m/z = 1137.28; determined m/z = 1137.28.

$[Pt_2I_2Me_6(L4)]$, 8. To a solution of complex **4** (0.010 g, 0.0082 mmol) in acetone-d_6 (0.5 mL) in an NMR tube was added MeI (1.2 µL, 0.0164 mmol). Immediately, on shaking, the bright red color of the mixture became pale yellow. ^{1}H NMR spectra were collected after 10 min., 1 h, 24 h. and 48 h. and indicated the formation of two isomers **8a** and **8b**. Addition of pentane precipitated the product as a yellow solid (Yield 74%), which was recrystallized from acetone/pentane to give single crystals of **8a**. NMR in acetone-d_6: **8a**, $\delta(^1H)$ 0.44 (s, ^2J(PtH) = 72 Hz, 6H, PtMe), 1.13 (s, ^2J(PtH) = 70 Hz, 6H, PtMe), 1.41 (s, 18H, ^{t}Bu), 1.46 (s, ^2J(PtH) = 70 Hz, 6H, PtMe), 1.79 (s, 6H, Me), 7.43 (d, ^3J(HH) = 9 Hz, 4H, H2b), 7.80 (d, ^3J(HH) = 9 Hz, 4H, H3b), 7.83 (dd, ^3J(HH) = 8 Hz, 5 Hz, 2H, H5a), 7.84 (s, 2H, H3), 7.87 (t, ^3J(HH) = 8 Hz, 2H, H4a), 7.91 (s, 2H, H1), 8.27 (d, ^3J(HH) = 8 Hz, 2H, H3a), 9.02 (d, ^3J(HH) = 5 Hz, ^3J(PtH) = 17 Hz, 2H, H6a), 9.43 (s, ^3J(PtH) = 27 Hz, 2H, Hi), 10.02 (s, 2H, NH); **8b**, $\delta(^1H)$ 0.61 (s, ^2J(PtH) = 72 Hz, 6H, PtMe), 1.21 (s, ^2J(PtH) = 70 Hz, 6H, PtMe), 1.41 (s, 18H, ^{t}Bu), 1.46 (s, ^2J(PtH) = 70 Hz, 6H, PtMe), 1.75, 1.80 (each s, 3H, Me), 7.56 (d, ^3J(HH) = 9 Hz, 4H, H2b), 7.83 (d, ^3J(HH) = 9 Hz, 4H, H3b), 7.83 (dd, ^3J(HH) = 8 Hz, ^3J(HH) = 5 Hz, 2H, H5a), 7.88 (s, 2H, H3), 7.96 (s, 2H, H1), 8.23 (t, ^3J(HH) = 8 Hz, 2H, H4a), 8.37 (d, ^3J(HH) = 8 Hz, 2H, H3a), 9.01 (d, ^3J(HH) = 5 Hz, ^3J(PtH) = 17 Hz, 2H, H6a), 9.31 (s,

^3J(PtH) = 27 Hz, 2H, Hi), 10.12 (s, 2H, NH). ESI-MS: Calc. for $[C_{55}H_{66}N_6O_3IPt_2]^+$ m/z = 1375.35; determined m/z = 1375.36.

$[Pt_2Br_2Me_4(CH_2Ph)_2(L3)]$, 9. To a stirred solution of complex **3** (0.020 g, 0.0204 mmol) in acetone (5 mL) was added $PhCH_2Br$ (4.8 µL, 0.0408 mmol). After 3 h., the solvent was evaporated *in vacuo*, to give the product as a yellow oily solid, which was dissolved in the minimum volume of CH_2Cl_2, precipitated by addition of pentane, and dried under vacuum. Yield 92%. NMR in CD_2Cl_2 : δ(^{1}H) 1.10 (s, ^2J(PtH) = 70 Hz, 6H, PtMe), 1.40 (s, 18H, ^{t}Bu), 1.53 (s, ^2J(PtH) = 71 Hz, 6H, PtMe), 1.80 (s, 6H, Me), 2.77 (d, ^2J(HH) = 9 Hz, ^2J(PtH) = 102 Hz, 2H, CH_2^A), 3.34 (d, ^2J(HH) = 9 Hz, ^2J(PtH) = 96 Hz, 2H, CH_2^B), 6.57 (d, ^3J(HH) = 7 Hz, 4H, Ho), 6.61 (t, ^3J(HH) = 7 Hz, 4H, Hm), 6.70 (t, ^3J(HH) = 7 Hz, 2H, Hp), 6.91 (dd, ^3J(HH) = 5 Hz, 7 Hz, 2H, H5a), 7.06 (t, ^3J(HH) = 7 Hz, 2H, H4a), 7.35 (d, ^4J(HH) = 2 Hz, 2H, H3), 7.51 (d, ^4J(HH) = 2 Hz, 2H, H1), 7.96 (d, ^3J(HH) = 7 Hz, 2H, H3a), 8.08 (d, ^3J(HH) = 5 Hz, ^3J(PtH) = 15 Hz, 2H, H6a), 9.83 (s, ^3J(PtH) = 27 Hz, 2H, Hi). ESI-MS: Calc. for $[C_{53}H_{64}BrN_4OPt_2]^+$ m/z = 1241.36; determined m/z = 1241.35.

$[Pt_2I_4Me_4(L3)]$, 10. To a stirred solution of complex **3** (0.020 g, 0.0204 mmol) in CH_2Cl_2 (5 mL) was added iodine (0.0103 g, 0.0408 mmol) in CH_2Cl_2 (2 mL). After 1 h., the volume of solvent was reduced under vacuum and the yellow product was precipitated by addition of pentane, separated by filtration and dried under vacuum. Yield 77%. NMR in CD_2Cl_2 : δ(^{1}H) 1.37 (s, 18H, ^{t}Bu), 1.79 (s, 6H, Me), 2.11 (s, ^2J(PtH) = 73 Hz, 6H, PtMe), 2.45 (s, ^2J(PtH) = 75 Hz, 6H, PtMe), 7.48 (dd, ^3J(HH) = 7 Hz, ^3J(HH) = 5 Hz, 2H, H5a), 7.50 (d, ^4J(HH) = 2 Hz, 2H, H3), 7.56 (t, ^3J(HH) = 7 Hz, 2H, H4a), 7.89 (d, ^4J(HH) = 2Hz, 2H, H1), 8.18 (d, ^3J(HH) = 7 Hz, 2H, H3a), 8.95 (d, ^3J(HH) = 5 Hz, ^3J(PtH) = 19 Hz, 2H, H6a), 9.65 (s, ^3J(PtH) = 30Hz, 2H, Hi). ESI-MS: Calc. for $[C_{39}H_{50}I_3N_4OPt_2]^+$ m/z = 1361.04; determined m/z = 1361.04.

$Pt_2Br_2(\mu_2\text{-}Hg)Me_4(L3)$], 11. To a solution of complex **3** (0.010 g, 0.0102 mmol) in acetone-d_6 (1 mL) in an NMR tube was added $HgBr_2$ (0.0037 g, 0.0102 mmol). The tube was sonicated for 15 min. to give an orange solution with a suspended orange solid. The NMR spectrum was recorded, the the mixture was added to pentane to give the product as an orange solid, which was separated by filtration, washed with pentane and dried under vacuum. Yield 81%. NMR in CD_2Cl_2: δ(^{1}H) 1.01 (s, ^2J(PtH) = 62 Hz, ^3J(HgH) = 12 Hz, 6H, PtMe), 1.37 (m, 18H, ^{t}Bu), 1.51 (s, ^2J(PtH) = 62 Hz, ^3J(HgH) = 12 Hz, 6H, PtMe), 1.78 (s, 3H, Me), 1.88 (s, 3H, Me), 7.59 (d, ^4J(HH) = 2Hz, 2H, H3), 7.62 (d, ^4J(HH) = 2Hz, 2H, H1), 7.72 (dd, ^3J(HH) = 7 Hz, ^3J(HH) = 5 Hz, 2H, H5a), 8.10 (d, ^3J(HH) = 7 Hz, 2H, H3a), 8.19 (t, ^3J(HH) = 7 Hz, 2H, H4a), 8.90 (d, ^3J(HH) = 5 Hz, ^3J(PtH) = 18 Hz, 2H, H6a), 9.25 (s, ^3J(PtH) = 26 Hz, 2H, Hi). ESI-MS: Calc. for $[C_{39}H_{51}BrN_4OHgPt_2]^+$ m/z = 1261.22; determined m/z = 1261.21.

$[Pt_2Me_6(\mu\text{-}C_4H_4N_2)(L3)][O_3SCF_3]_2$, 12. To a stirred solution of complex **7** (0.010 g, 0.0088 mmol) in acetone (5 mL) was added AgO_3SCF_3 (0.0044 g, 0.0176 mmol). After 1 h., pyrazine (0.0008 g, 0.0044 mmol) was added and the mixture was stirred for 1 h. The mixture was filtered to remove AgI, then the solvent was evaporated, and the yellow solid product was washed with pentane and dried under vacuum. Yield 81%. NMR in CD_2Cl_2: δ(^{1}H) 1.01 (s, ^2J(PtH) = 72 Hz, 6H, PtMe), 1.27 (s, ^2J(PtH) = 68 Hz, 6H, PtMe), 1.42 (s, 18H, ^{t}Bu), 1.48 (s, ^2J(PtH) = 70 Hz, 6H, PtMe), 1.65 (s, 3H, Me), 2.04 (s, 3H, Me), 7.15 (d, ^4J(HH) = 2 Hz, 2H, H3), 7.67 (d, ^4J(HH) = 2 Hz, 2H, H1), 7.94 (dd, ^3J(HH) = 7 Hz, 5 Hz, 2H, H5a), 8.14 (t, ^3J(HH) = 7 Hz, 2H, H4a), 8.20 (s, ^3J(PtH) = 10 Hz, 2H, H_{pz}), 8.63 (d, ^3J(HH) = 7 Hz, 2H, H3a), 8.75 (s, ^3J(PtH) = 10 Hz, 2H, H_{pz}), 8.91 (d, ^3J(HH) = 5 Hz, ^3J(PtH) = 18 Hz, 2H, H6a), 9.49 (s, ^3J(PtH) = 26 Hz, 2H, Hi). ESI-MS: Calc. for $[C_{45}H_{60}N_6OPt_2]^{2+}$ m/z = 545.21; determined m/z = 545.21.

$[Pt_2Me_6(C_4H_4N_2)(L4)][O_3SCF_3]_2$, 13. This was prepared similarly but using complex **8**. Yield 92%. NMR in acetone-d_6: δ(^{1}H) 0.86 (s, ^2J(PtH) = 72 Hz, 6H, PtMe), 1.06 (s, ^2J(PtH) = 68 Hz, 6H, PtMe), 1.31 (s, ^2J(PtH) = 68 Hz, 6H, PtMe), 1.41 (s, 18H, ^{t}Bu), 1.78 (s, 3H, Me), 1.80 (s, 3H, Me), 7.31 (d, ^3J(HH) = 9 Hz, 4H, H2b), 7.91 (s, 2H, H3), 8.07 (s, 2H, H1), 8.07 (dd, ^3J(HH) = 8Hz, ^3J(HH) = 5Hz, 2H, H5a), 8.33 (d, ^3J(HH) = 9Hz, 4H, H3b), 8.46 (m, 4H, H3a/H4a), 8.54 (s, 4H, Hpz), 9.09 (d, ^3J(HH) = 5Hz, ^3J(PtH) = 18 Hz, 2H, H6a), 9.40 (s, ^3J(PtH) = 27 Hz, 2H, Hi), 10.26 (s, 2H, NH). ESI-MS: Calc. for $[C_{59}H_{70}N_8O_3Pt_2]^{2+}$ m/z = 664.24; determined m/z = 664.23.

CONFLICTS OF INTEREST

The authors have declared that there is no conflict of interest.

ACKNOWLEDGMENTS

We thank the NSERC (Canada) for financial support and Dr. P.D. Boyle for assistance with structure determinations.

SUPPLEMENTARY INFORMATION

Crystallographic data for the structural analysis have been deposited with the Cambridge Crystallographic Data Centre (CCDC 2145542-2145544). Copies of this information may be obtained free of charge from: The Director, CCDC, 12 Union Road, Cambridge, CB2 1EZ, UK. Fax: +44(1223)336-033, e-mail: deposit@ccdc.cam.ac.uk, or www.ccdc.cam.ac.uk. Figures S1-S13 showing NMR spectra of the complexes. The file xyz.xyz contains the calculated atomic coordinates of the complexes from DFT calculations.

AUTHOR INFORMATION

Corresponding Author

Richard J. Puddephatt: Email: pudd@uwo.ca, *ORCID*: 0000-0002-9846-3075

Author

Matthew S. McCready

REFERENCES

1. B. I. Kharisov, P. E. Martinez, V. M. Jimenez-Perez, O. V. Kharissova, B. N. Martinez, N. Perez, *J. Coord. Chem.* **2010**, *63*, 1-25.
2. P. J. Steel, *Acc. Chem. Res.* **2005**, *38*, 243-250.
3. C. Kaes, A. Katz, M. W. Hosseini, *Chem. Rev.* **2000**, *100*, 3553-3590.
4. R. Ziessel, M. Hissler, A. El-Ghayoury, A. Harriman, *Coord. Chem. Rev.* **1998**, *178*, 1251-1298.
5. A. L. Gavrilova, B. Bosnich, *Chem. Rev.* **2004**, *104*, 349-383.

6. C. Uyeda, C. M. Farley, *Acc. Chem. Res.* **2021**, *54*, 3710-3719.
7. E. K. van den Beuken, B. L. Feringa, *Tetrahedron* **1998**, *54*, 12985-13011.
8. M. Shibasaki, M. Kanai, S. Matsunaga, N. Kumagai, *Acc. Chem. Res.* **2009**, *42*, 1117-1127.
9. P. J. Lusby, P. Muller, S. J. Pike, A. M. Z. Slawin, *J. Am. Chem. Soc.* **2009**, *131*, 16398-16400.
10. D. Schilter, J. K. Clegg, M. M. Harding, L. M. Rendina, *Dalton Trans.* **2010**, *39*, 239-247.
11. A. Baba, T. Kojima, S. Hiraoka, *J. Am. Chem. Soc.* **2015**, *137*, 7664-7667.
12. J. H. H. Ho, S. W. S. Choy, S. A. Macgregor, B. A. Messerle, *Organometallics* **2011**, *30*, 5978-5984.
13. M. G. Timerbulatova, M. R. D. Gatus, K. Q. Vuong, M. Bhadbhade, A. G. Algarra, S. A. Macgregor, B. A. Messerle, *Organometallics* **2013**, *32*, 5071-5081.
14. E. A. Wood, L. F. Gildea, D. S. Yufit, J. A. G. Williams, *Polyhedron* **2021**, *207*, 115401.
15. J. Hu, H. Xu, M. H. Nguyen, J. H. K. Yip, *Inorg. Chem.* **2009**, *48*, 9684-9692.
16. Z. Guo, W. -L. Tong, M. C. W. Chan, *Chem. Commun.* **2009**, 6189-6191.
17. W. -L. Tong, S. -M. Yiu, M. C. W. Chan, *Inorg. Chem.* **2013**, *52*, 7114-7124.
18. R. L. Hollingsworth, A. Bheemaraju, N. Lenca, R. L. Lord, S. Groysman, *Dalton Trans.* **2017**, *46*, 5605-5616.
19. A. Bheemaraju, J. W. Beattie, Y. Danylyuk, J. Rochford, S. Groysman, *Eur. J. Inorg. Chem.* **2014**, 5865-5873.
20. M. Crespo, M. Martinez, S. M. Nabavizadeh, M. Rashidi, *Coord. Chem. Rev.* **2014**, *279*, 115-140.
21. L. M. Rendina, R. J. Puddephatt, *Chem. Rev.* **1997**, *97*, 1735-1754.
22. R. B. Aghakhanpour, S. Paziresh, S. M. Nabavizadeh, S. J. Hoseini, F. N. Hosseini, *J. Iran. Chem. Soc.* **2020**, *17*, 2683-2715.
23. S. J. Hoseini, S. M. Nabavizadeh, S. Jamali, M. Rashidi, *Eur. J. Inorg. Chem.* **2008**, *32*, 5099-5105.
24. S. M. Nabavizadeh, M. D. Aseman, B. Ghaffari, M. Rashidi, F.N. Hosseini, G. Azimi, *J. Organomet. Chem.* **2012**, *715*, 73-81.
25. M. P. Brown, R. J. Puddephatt, M. Rashidi, *Inorg. Chim. Acta* **1976**, *19*, L33-L34.
26. M. P. Brown, A. Hollings, K. J. Houston, R. J. Puddephatt, M. Rashidi, *J. Chem. Soc. Dalton Trans.* **1976**, 786-791.
27. M. D. Aseman, M. Rashidi, S. M. Nabavizadeh, R. J. Puddephatt, *Organometallics* **2013**, *32*, 2593-2598.
28. G. S. Hill, M. J. Irwin, C. J. Levy, L. M. Rendina, R. J. Puddephatt, R. A. Andersen, L. McLean, *Inorg. Synth.* **1998**, *32*, 149-153.
29. J. D. Scott, R. J. Puddephatt, *Organometallics* **1983**, *2*, 1613-1618.
30. J. D. Scott, R. J. Puddephatt, *Organometallics* **1986**, *5*, 2522-2529.
31. M. Crespo, R. J. Puddephatt, *Organometallics* **1987**, *6*, 2548-2550.
32. S. Habibzadeh, M. Rashidi, S. M. Nabavizadeh, L. Mahmoodi, F. N. Hosseini, R. J. Puddephatt, *Organometallics* **2010**, *29*, 82-88.
33. R. J. Puddephatt, *Angew. Chem. Int. Ed.* **2002**, *41*, 261-263.
34. S. M. Nabavizadeh, H. Amini, M. Rashidi, K. R. Pellarin, M. S. McCready, B. F. T. Cooper, R. J. Puddephatt, *J. Organomet. Chem.* **2012**, *713*, 60-67.
35. M. C. Janzen, M. C. Jennings, R. J. Puddephatt, *Inorg. Chem.* **2001**, *40*, 1728-1729.
36. M. C. Janzen, M. C. Jennings, R. J. Puddephatt, *Inorg. Chim. Acta* **2005**, *358*, 1614-1622.
37. T. Yamaguchi, K. Yoshiya, *Inorg. Chem.* **2019**, *58*, 9548-9552.
38. V. Mishra, N. K. Sinha, N. Thirupathi, *Inorg. Chem.* **2021**, *60*, 3879-3892.
39. M. P. Brown, R. J. Puddephatt, M. Rashidi, *Inorg. Chim. Acta* **1977**, *23*, L33-L34.
40. Lj. Manojlovic-Muir, K. W. Muir, A. A. Frew, S. S. M. Ling, M. A. Thomson, R. J. Puddephatt, *Organometallics* **1984**, *3*, 1637-1645.
41. Bruker-AXS, SAINT, **2013**, Bruker-AXS, Madison, WI 53711, USA.
42. Bruker-AXS, TWINABS, **2012**, Bruker-AXS, Madison, WI 53711, USA.
43. G. M. Sheldrick, *Acta Cryst.* **2015**, *A71*, 3-8.
44. G. M. Sheldrick, *Acta Cryst.* **2015**, *C71*, 3-8.
45. A. D. Becke, *Phys. Rev. A* **1988**, *38*, 3098-3100.
46. J. Andzelm, C. Kolmel, A. Klamt, *J. Chem. Phys.* **1995**, *103*, 9312-9320.
47. ADF **2020**, SCM, Vrije Universiteit, Amsterdam, The Netherlands, http://www.scm.com.